ELSEVIER

Thermochimica Acta 330 (1999) 101–107

thermochimica acta

Quasi-isothermal measurement of frequency dependent heat capacity of semicrystalline polyethylene at the melting temperature using light heating modulated temperature DSC

Y. Saruyama

Faculty of Textile Science, Kyoto Institute of Technology, Matsugasaki, Sakyo-ku, Kyoto 606-8585, Japan

Received 3 August 1998; accepted 10 December 1998

Abstract

Frequency dependence of the heat capacity of semicrystalline polyethylene was measured using light heating modulated temperature DSC (LMDSC). The quasi-isothermal measurement was carried out in the melting temperature range of the crystal. Two decades of the frequency, from 0.01 to 1 Hz, was covered by the LMDSC instrument constructed in the author's laboratory. It was found that in the melting temperature range polyethylene exhibited Debye relaxation with the relaxation time of 14 s and had excess heat capacity independent of the kinetics. The excess heat capacity and the relaxation strength could be attributed to the disordered crystals generated during rapid cooling from the molten state and/or its surrounding amorphous region instead of the stable crystals reorganized during the quasi-isothermal measurement.

Keywords: Light heating modulated temperature DSC; LMDSC; Qausi-isothermal measurement; Polyethylene; Melting

1. Introduction

Modulated temperature differential scanning calorimetry (MTDSC) have been applied to the melting and the crystallization of polymers as well as the glass transition and irreversible phenomena. It was pointed out in the early works [1,2] that simple separation into the reversible and non-reversible components was not successful in the melting/crystallization temperature range. Recently new techniques to study the melting and the crystallization were proposed. Wunderlich et al. [3] carried out quasi-isothermal (zero underlying heating rate) measurement to eliminate the contribution from irreversible melting or crystallization from the superheated or supercooled state, respectively. Saruyama [4] measured frequency dependence of heat capacity of semicrystalline polyethylene around the melting temperature of the crystal using a light heating modulated temperature DSC (LMDSC) [5,6] and found that the frequency had to be equal to or higher than 0.1 Hz to obtain frequency independent results. Toda et al. [7,8] showed that the rate of crystal growth and melting could be estimated from frequency dependence of the heat capacity.

These works showed that MTDSC and LMDSC were useful to study the melting and the crystallization of polymers. In this study we carried out the quasi-isothermal measurement of semicrystalline polyethylene over two decades of the modulation frequency from 0.01 to 1 Hz. The purpose of this work was to investigate frequency dependence of the heat capacity obtained from the quasi-isothermal measurement.

0040-6031/99/$ – see front matter
PII: S0040-6031(99)00024-6

2. Experimental

2.1. Sample preparation

A thin disk of polyethylene (NIST 1475) was put in an aluminum pan and covered by an aluminum lid. Sample mass was 2.8 mg. The sample was melted in the DSC furnace with a small weight (1 g) on the lid in order to make the sample be in good contact with the pan and the lid. An aluminum pan to which a lid was fixed with a very small amount of grease was put on the reference side. The pans were not crimped to avoid deformation of the bottom of the pan. Carbon was sprayed over the upper surface of the lids for light absorption.

2.2. Instrumentation

The LMDSC instrument used in this work was constructed in our laboratory using a commercial heat flux type DSC instrument [5,6]. LMDSC has an advantage of wider frequency range (from 0.01 to 1 Hz) than commercial instruments (typically from 0.01 to 0.1 Hz). Another advantage of LMDSC is independent control of the light intensity of the sample and reference sides. This enables compensating for the asymmetry of the thermal system of the instrument as explained below.

Temperature profile of the quasi-isothermal measurement is shown in Fig. 1. The temperature was increased stepwise from 120°C to 131°C by an increment of one degree. The quasi-isothermal measurement was made for 1 h at each temperature. Crystallization on the cooling process occurred between 120°C and 110°C.

The modulation frequency was fixed during one scan of the temperature profile. After the frequency was changed at the end of the temperature profile the next scan started without delay. The measured frequency was 0.01, 0.02, 0.05, 0.1, 0.2, 0.5 and 1 Hz. Integral time for Fourier transform was 200, 100, 40 and 20 s for 0.01, 0.02, 0.05 and 0.1 Hz and higher, respectively. Measurement at 0.1 Hz was carried out two times, the first and last scans, to check reproducibility. Both the sample and reference sides were modulated by the light. Amplitude of the temperature modulation of each side was a few hundred mK or less. Measurement at a constant underlying heating rate, 3 K/min, was made to obtain the total heat flow without the annealing effects.

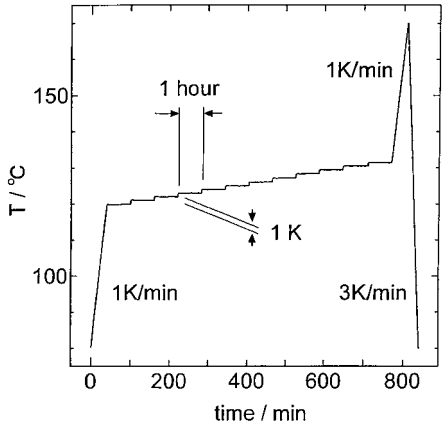

Fig. 1. Temperature profile of the quasi-isothermal measurement.

Another type of measurement was carried out modulating only the reference side. A material of the sample side was replaced with what was similar to that of the reference side. Temperature was changed at a constant underlying heating rate. Modulation frequencies studied were the same with those of the quasi-isothermal measurement.

2.3. A mathematical model for the thermal system

In this section two things will be explained on the basis of a mathematical model for the thermal system; the first is how asymmetry of the instrument was compensated for and the second is how the heat capacity was calculated from the measured quantities. Fig. 2 shows a model for LMDSC. Asymmetry of the thermal system was taken into account. A basic equation for the sample side was given by the next equation

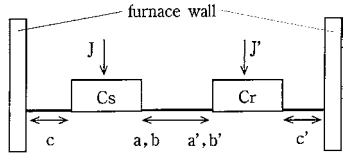

Fig. 2. A model for the thermal system of LMDSC. C_s: heat capacity of the sample side, C_r: heat capacity of the reference side, J, J': energy flow of the light, a, a', b, b', c, c': complex machine constant characterizing heat exchange.

using complex machine constants [9].

$$C_s\dot{T}_s = J - aT_s + bT_r - cT_s, \quad (1)$$

where C_s and T_s are heat capacity of a material of the sample side composed of the sample, the pan, the lid, the detector and the complex amplitude of the temperature modulation, respectively. It was assumed that there was no temperature difference in the material. Time derivative of temperature expressed by $\dot{T}_s$ can be rewritten as $i\omega T_s$, where ω is angular frequency of the modulation. The letter J denotes the complex amplitude of the energy flow of the light. Complex constants, a, b and c, characterize heat exchange between the sample and reference sides (a, b) and the material and the furnace wall (c), respectively. A basic equation for the reference side was obtained from Eq. (1) by replacing the subscript s/r with r/s and J, a, b and c with J', a', b' and c', respectively.

$$C_r\dot{T}_r = J' - a'T_r + b'T_s - c'T_r. \quad (2)$$

Since the basic equations were linear equations for T_s and T_r, it was straightforward to solve them. The temperature difference, $\Delta T = T_s - T_r$, was calculated from the solution.

$$\Delta T = \frac{(i\omega C_r + a' + c' - b')J - (i\omega C_s + a + c - b)J'}{(i\omega C_s + a + c)(i\omega C_r + a' + c') + bb'}. \quad (3)$$

We considered two cases, that is, ($J \neq 0$, $J' \neq 0$) and ($J \neq 0$, $J' = 0$). The ratio of ΔT of the first case to that of the second case was given by

$$\frac{\Delta T(J \neq 0,\ J' \neq 0)}{\Delta T(J \neq 0,\ J' = 0)} = 1 - \frac{i\omega C_s + a + c - b}{i\omega C_r + a' + c' - b'}\frac{J'}{J}. \quad (4)$$

Using the heat capacity difference, $C_{sr} = C_s - C_r$, the next equation was obtained.

$$\frac{\Delta T(J \neq 0,\ J' \neq 0)}{\Delta T(J \neq 0,\ J' = 0)} = 1 - \frac{i\omega C_r + a + c - b}{i\omega C_r + a' + c' - b'}\frac{J'}{J} - \frac{i\omega}{i\omega C_r + a' + c' - b'}\frac{J'}{J}C_{sr}. \quad (5)$$

It can be seen from Eq. (5) that if the system is asymmetric C_{sr} is not proportional to the left-hand side of Eq. (5) since the second term of the right-hand side is not unity. However, in LMDSC J and J' can be controlled independently. Putting pans of same mass on the sample and reference sides light intensity of the reference side was adjusted to make the temperature difference between the sample and reference sides minimum. Since the thermal system became effectively symmetric the next equation was used to calculate the heat capacity from the measured quantities.

$$\frac{\Delta T(J \neq 0,\ J' \neq 0)}{\Delta T(J \neq 0,\ J' = 0)} = KC_{sr}, \quad (6)$$

where K is the coefficient of the third term of the right-hand side of Eq. (5). The numerator of the left-hand side of Eq. (6) was directly obtained from the quasi-isothermal measurement. On the other hand the denominator was calculated using the next equation.

$$\Delta T(J \neq 0,\ J' = 0) = \Delta T(J \neq 0,\ J' \neq 0) - \Delta T(J = 0,\ J' \neq 0). \quad (7)$$

The first term of the right-hand side is the same with the numerator. The second term was obtained from the measurement with a constant underlying heating rate. The results from the constant underlying heating rate measurement were fitted by a quadratic function of temperature and the calculated values from the quadratic function were used for data analysis. This method reduced noise from the constant underlying heating rate measurement. It should be noted that the phase of the first and second terms of the right-hand side of Eq. (7) must be measured relative to a standard signal common to the both terms. Light intensity was monitored with a photo-diode and used as the standard. In our method two separate measurements were necessary to estimate the numerator and the denominator. On the other hand commercial instruments give two independent signals by one measurement, the differential signal and the sample temperature. However, the advantage of our method is that both the numerator and the denominator are obtained from differential signals. The signal to noise ratio of the small cyclic component extracted from the large signal of the sample temperature is not so good as that of the cyclic component extracted from the differential signal.

The calibration parameter K depends on both temperature and frequency. Temperature dependence of K was approximated by a linear function, which was determined to make the experimental value of C_{sr} fit the ATHAS data [10] between 80°C and 100°C assum-

ing 75% of crystallinity. The linear function was determined for each frequency.

It was found that the linear approximation for K could not be extended to temperatures higher than the end point of melting. The values of C_{sr} in the molten state calculated from the linear approximation for K exhibited linear temperature dependence with a good signal to noise ratio. However, the slope of the linear temperature dependence was different from a temperature scan to another and the values of C_{sr} scattered in the range ±17% around the average value at 150°C. Systematic frequency dependence was not observed. On the other hand reasonable frequency dependence was observed for temperatures lower than the end point of melting as will be shown in Section 3. We assumed that the linear approximation for K was successful before the end point of melting but it failed suddenly after the melting was finished. A possible origin of this sudden change was change in thermal contact between the sample and the pan and/or the lid at the final stage of melting where the sample began to flow. It was considered that the thermal contact of the molten state was same in every temperature scan but that of the solid state was different from one temperature scan to another. The scattered values of C_{sr} suggested that quality of the thermal contact of the solid state could not be controlled only by the cooling rate from the molten state.

3. Results

As pointed out by Birge [11] heat capacity characterizing cyclic temperature change due to cyclic heat absorption depends on the frequency. This heat capacity should be expressed by a complex number because it determines the phase of the temperature change as well as the amplitude. The complex heat capacity will be denoted by $C(\omega)$ below. In this work $C(\omega)$ was equal to C_{sr} since the difference between the materials on the sample and reference sides was only the sample disk.

Fig. 3 shows time dependence of $|C(\omega)|$ at 0.01, 0.1 and 1 Hz during the quasi-isothermal measurement at (129.3±0.1)°C. Data points show the calculated values at every 10 s. In this paper we show only the results of $|C(\omega)|$ because reproducibility of the phase of $C(\omega)$ was not good enough. The poor reproducibility of the phase was considered to be due to the uncontrollable thermal contact between the sample and the pan and/or the lid. Fig. 3 shows gradual but steady decrease of $|C(\omega)|$. Similar decrease was observed at other frequencies and temperatures. Although the decrease of $|C(\omega)|$ did not finish after 1 h, the results between 2000 and 3000 s were averaged in order to examine temperature and frequency dependence.

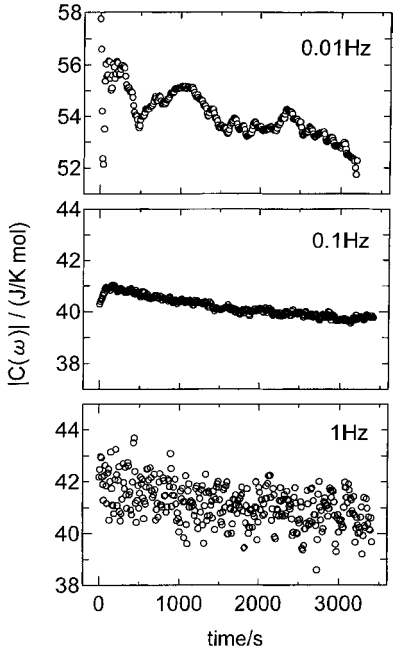

Fig. 3. Time dependence of $|C(\omega)|$ during the quasi-isothermal measurement at (129.3±0.1)°C. The modulation frequency is given in the figure.

Fig. 4 shows temperature dependence of the averaged $|C(\omega)|$ at various frequencies. $|C(\omega)|$ was notably dependent on the frequency in the low frequency range. On the other hand at frequencies equal to or higher than 0.1 Hz $|C(\omega)|$ was almost independent of the frequency. It can be seen from Fig. 4 that the ratio of $(|C(0.01\,\mathrm{Hz})| - |C(0.1\,\mathrm{Hz})|)$ to $(|C(0.02\,\mathrm{Hz})| - |C(0.1\,\mathrm{Hz})|)$ is almost independent of temperature. Taking account of this result we assumed that $C(\omega)$ could be expressed by the next equation.

$$C(\omega) = C(\infty) + \Delta C \frac{1}{1 + i\omega\tau}, \tag{8}$$

where $C(\infty)$ and ΔC were dependent on only tem-

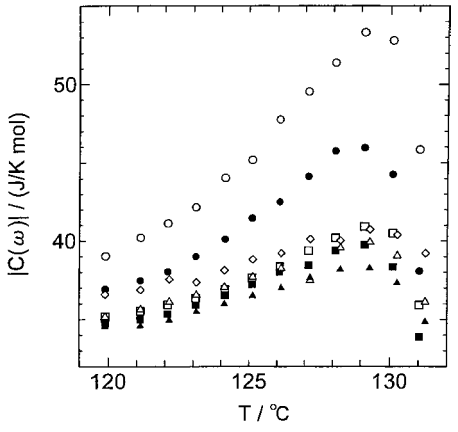

Fig. 4. Temperature dependence of $|C(\omega)|$: (○) 0.01 Hz, (●) 0.02 Hz, (□) 0.05 Hz, (■) 0.1 Hz, (△) 0.2 Hz, (▲) 0.5 Hz, (◇) 1 Hz.

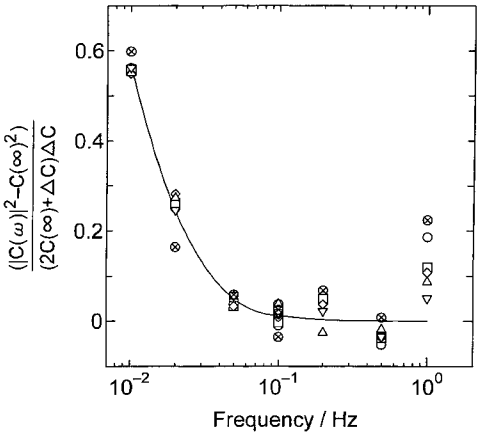

Fig. 5. Fitting of the curve calculated according to the model of Debye relaxation to the measured date. (○) 121°C, (□) 123°C, (◇) 125°C, (△) 127°C, (▽) 129°C, (⊗) 131°C.

perature. Since $C(\infty)$ and ΔC were heat capacity without the contribution from the kinetics and the relaxation strength, respectively, they were expressed by real numbers. The frequency dependent part was given by Debye function. Relaxation time τ was assumed to be independent of both temperature and frequency. From Eq. (8) the next equation was obtained.

$$|C(\omega)|^2 = C(\infty)^2 + (2C(\infty) + \Delta C)\Delta C \times \frac{1}{1+\omega^2\tau^2}. \quad (9)$$

Values of τ, $C(\infty)$ and ΔC were determined by the following procedure:

1. A value of τ was given.
2. Values of $C(\infty)^2$ and $(2C(\infty) + \Delta C)\ \Delta C$ were determined at each temperature to fit the calculated values of the right-hand side of Eq. (9) to the experimental results of the left-hand side.
3. The square sum of the difference between the calculated and experimental values was minimized by repeating the processes (1) and (2) assuming various values of τ.

Fig. 5 shows frequency dependence of $(|C(\omega)|^2 - C(\infty)^2)/(2C(\infty) + \Delta C)\Delta C$ which is expected to be independent of temperature from Eq. (9). Experimental results at every other temperature of the quasi-isothermal measurement are shown in Fig. 5 to avoid confusion of the data points. The data points at 0.1 Hz show two sets of results from the first and last scans of the temperature profile shown in Fig. 1. It can be seen that reproducibility of the measurement was sufficiently good. The curve in Fig. 5 was calculated from $1/1 + \omega^2\tau^2$ with τ=14 s. The calculated curve agreed well with the experimental results except the points at 1 Hz; the data obtained at 1 Hz were not used in the

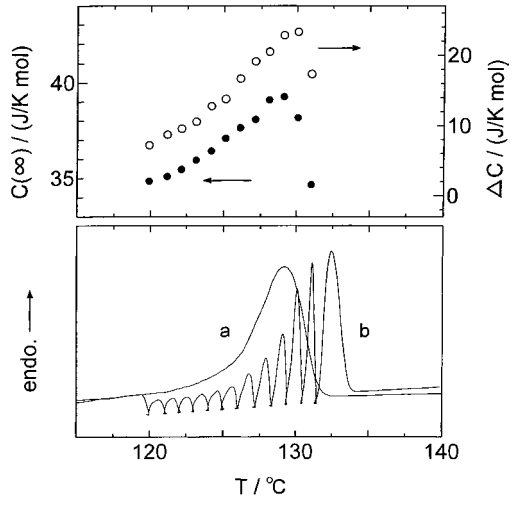

Fig. 6. Temperature dependence of $|C(\infty)|$ and ΔC and total heat flow curves. Curve a: measurement at a constant underlying heating rate (3 K/min), curve b: quasi-isothermal measurement.

second process of the fitting procedure. Temperature dependence of $C(\infty)$ and ΔC is shown in Fig. 6 with the total heat flow curves of (a) a constant underlying heating rate measurement at 3 K/min and (b) the quasi-isothermal measurement.

4. Discussion

The decrease of $|C(\omega)|$ shown in Fig. 3 is consistent with the result of a previous study on the crystallization of polyethylene [12]. This decrease can be attributed to change in the heat capacity due to annealing just below the melting temperature. Signal quality is best at 0.1 Hz. The large noise level of the results of 1 Hz is due to the small amplitude of the cyclic component. As can be seen in Fig. 5 the results of 1 Hz are notably deviated from the calculated curve. This deviation suggests that thermal contact between the sample and the pan and/or the lid was not good enough for measurement at a high frequency. Origin of the slow but large fluctuation of the results of 0.01 Hz has not been understood yet.

Good agreement of the observed points with the calculated curve in Fig. 5 shows validity of the model of Eq. (8) which means that polyethylene exhibits Debye relaxation at the melting temperature. Temperature dependence of the relaxation time was weak enough to be neglected in the melting temperature range. Temperature dependence of $C(\infty)$ and ΔC shown in Fig. 6 has a peak around 129°C. The value of $C(\infty)$ is larger than the heat capacity of the amorphous state (35 J/K mol at 130°C [10]). Since the peak of $C(\infty)$ cannot be attributed to the thermal vibration there must be excess heat capacity in the melting temperature range. It should be noted that the peak positions are close to that of the curve a of the total heat flow instead of the curve b although $C(\infty)$ and ΔC were measured simultaneously with the curve b. Polymer crystals generated during rapid cooling from the molten state are disordered and far from the equilibrium state. The disordered crystal can be converted to a more stable state by reorganization and/or melting and recrystallization during annealing just below the melting temperature. Shift of the total heat flow curve from the curve a to b is due to the conversion to more stable states. The heating rate of 3 K/min is fast enough for the polyethylene crystal to avoid the annealing effects. Therefore, it seems that $C(\infty)$ and ΔC are caused by the disordered crystals which were not converted to the more stable states.

There are two possible parts of the sample to which ΔC and the excess heat capacity in $C(\infty)$ can be attributed; one is the disordered crystals and the other is amorphous region around the disordered crystals. In semicrystalline polymers there are molecules a part of which belongs to the crystal and the rest of which is in the amorphous state. If there are a number of such molecules around the disordered crystals the surrounding amorphous region can be strongly affected by the molecules and have heat capacity different from that of the ideal amorphous state. It should be remembered that there is no reason to say that the excess heat capacity and ΔC should be attributed to the same part of the sample. The degree of freedom related to the excess heat capacity can exchange energy with the thermal vibration rapidly enough to follow the modulation at 1 Hz, while the energy exchange between the degree of freedom related to ΔC and the thermal vibration is too slow to follow the modulation. It seems to be reasonable that the part of the sample related to the rapid energy exchange is different from the part related to the slow energy exchange. More detailed studies will be necessary to determine the origin of the excess heat capacity and ΔC.

It is stressed that the measurement of frequency dependence over a wide frequency range was essential to obtain the above results. On the other hand simultaneous measurement of $C(\omega)$ and the total heat flow was very important for comparing in Fig. 6. It can be said that LMDSC is a useful technique to satisfy the both requirements.

References

[1] P.S. Gill, S.R. Sauerbrunn, M. Reading, J. Therm. Anal. 40 (1993) 931.
[2] M. Reading, D. Elliott, V.L. Hill, J. Therm. Anal. 40 (1993) 949.
[3] B. Wunderlich, I. Okazaki, K. Ishikiriyama, A. Boller, Proceedings of the 25th NATAS Conference, 1997, p. 49.
[4] Y. Saruyama, Thermochim. Acta 304–305 (1997) 171.
[5] Y. Saruyama, Proceedings of the 25th NATAS conference, 1997, p. 700.
[6] Y. Saruyama, J. Therm. Anal. 54 (1998) 687.

[7] A. Toda, C. Tomita, T. Oda, M. Hikosaka, Y. Saruyama, Proceedings of the 25th NATAS conference, 1997, p. 645.
[8] A. Toda, C. Tomita, M. Hikosaka, Y. Saruyama, Proceedings of the 25th NATAS conference, 1997, p. 659.
[9] Y. Saruyama, Thermochim. Acta 283 (1996) 157.
[10] U. Gaur, B. Wunderlich, J. Phys. Chem. Ref. Data 10 (1981) 119.
[11] N.O. Birge, Phys. Rev. B34 (1986) 1631.
[12] A. Toda, T. Oda, M. Hikosaka, Y. Saruyama, Thermochim. Acta 293 (1997) 47.